this does not occur shows that selenium is not available for abstraction because it is all strongly coordinated to cadmium, thus confirming the conclusions drawn earlier that it is the cadmium-phosphorus bond which is labile in $[Cd(dpmSe)_2]^{2+}$.

Conclusions

The results presented in this paper clearly support the concept of the group 16 donor atoms, sulfur and selenium, being more strongly coordinated to cadmium(II) than phosphorus, in contrast to the earlier conclusions[14] that mercury prefers coordination to phosphorus.

There is an apparent anomaly in that stability constants calculated for the dpmE and $dpmE_2$ complexes of cadmium(II) by the use of electrochemical methods in dichloromethane show that the dpmE ligands, which are capable of forming Cd–P bonds, form the most stable complexes. However, a consideration of the ligand geometries resolves this anomaly. DpmE ligands are not as flexible as the $dpmE_2$ ligands, and consequently, the dpmE ligands form chelates much more readily because when selenium or sulfur is coordinated, the phosphorus is close to the metal. The magnitude of these stability constants suggests that all of the dpmE and $dpmE_2$ complexes of cadmium(II) are completely nondissociated in solution.

The $dpmE_2$ complexes only possess a coordination number of 4 even at high cadmium to ligand ratios, whereas the stronger dpmE complexes have coordination numbers of 6 at high ligand concentrations. At these high cadmium to ligand ratios complexes of the type $[Cd(\eta^1\text{-dpmE})_6]^{2+}$ are assumed in which the ligand is coordinated in a monodentate fashion through the group 16 donor atom.

The calculated stability constants also reveal that the selenium-containing ligands form stronger complexes than their sulfur analogues. This is in accordance with other studies involving sulfur and selenium ligands, in particular that of $[Hg(dpmE)_2]^{2+}$ and $[Hg(dpmE_2)_2]^{2+}$, in which the sulfur derivatives are easier to reduce than their selenium analogues.[14]

Acknowledgment. We are indebted to Professor R. H. Philp, Jr., for helpful discussions. J.E. thanks the Commonwealth Government of Australia for a Postgraduate Research Award.

Registry No. dpmSe, 23176-19-4; dpmS, 54006-28-9; $dpmSe_2$, 16675-12-0; $dpmS_2$, 14633-92-2; $[Cd(dpmSe)_2][ClO_4]_2$, 123506-14-9; $[Cd(dpmS)_2][ClO_4]_2$, 123506-16-1; $[Cd(dpmSe)_2][CF_3SO_3]_2$, 123506-17-2; $[Cd(dpmS)_2][CF_3SO_3]_2$, 123506-18-3; $[Cd(dpmSe_2)_2][ClO_4]_2$, 123540-25-0; $[Cd(dpmS_2)_2][ClO_4]_2$, 123565-35-5; PPh_3, 603-35-0; PPh_3Se, 3878-44-2; $[Hg(dpe)_2][ClO_4]_2$, 123540-05-6; ^{77}Se, 14681-72-2; ^{113}Cd, 14336-66-4; $[Cd(\eta^1\text{-dpmSe})_6]^{2+}$, 123506-19-4; $[Cd(\eta^1\text{-dpmS})_6]^{2+}$, 123506-20-7; $[Cd(DMSO)_6][CF_3SO_3]_2$, 76703-11-2.

Supplementary Material Available: Tables S-I–S-VII, listing dc polarographic data for the oxidation of a Cd(Hg) amalgam electrode in the presence of $dpmE_2$, dpmS, PPh_3, and PPh_3Se and reduction of $[Cd(PPh_3)_x]^{2+}$ and $[Cd(PPh_3Se)_4]^{2+}$ at a dropping-mercury electrode (8 pages). Ordering information is given on any current masthead page.

Contribution from the Department of Chemistry, North Carolina State University, Raleigh, North Carolina 27695-8204,
Chemistry and Materials Science Divisions, Argonne National Laboratory, Argonne, Illinois 60439,
and Sandia National Laboratories, Albuquerque, New Mexico 87185

Similarities and Differences in the Structural and Electronic Properties of κ-Phase Organic Conducting and Superconducting Salts

D. Jung,[†] M. Evain,[†] J. J. Novoa,[†] M.-H. Whangbo,[*,†] M. A. Beno,[‡] A. M. Kini,[‡] A. J. Schultz,[‡]
J. M. Williams,[*,‡] and P. J. Nigrey[§]

Received April 25, 1989

We have examined the similarities and differences in the crystal and band electronic structures of four κ-phase tetrathiafulvalene-based organic conducting salts κ-$(BEDT\text{-}TTF)_2X$ ($X^- = Cu(NCS)_2^-, I_3^-$), κ-$(MDT\text{-}TTF)_2AuI_2$, and κ-$(BMDT\text{-}TTF)_2Au(CN)_2$. Donor dimers have a bond-over-ring arrangement in the superconducting salts κ-$(BEDT\text{-}TTF)_2X$ ($X^- = Cu(NCS)_2^-, I_3^-$) and κ-$(MDT\text{-}TTF)_2AuI_2$ but a bond-over-bond arrangement in the nonsuperconducting salt κ-$(BMDT\text{-}TTF)_2Au(CN)_2$, so that the intradimer spacing is considerably larger in the nonsuperconducting than in the superconducting κ-phases. The terminal ethylene groups of BEDT-TTF have a staggered arrangement in the "high-T_c" salts κ-$(BEDT\text{-}TTF)_2Cu(NCS)_2$ (T_c = 10.4 K) and β*-$(BEDT\text{-}TTF)_2I_3$ (T_c = ~ 8 K) but are eclipsed in the "low-T_c" salts κ-$(BEDT\text{-}TTF)_2I_3$ (T_c = 3.6 K), β-$(BEDT\text{-}TTF)_2AuI_2$ (T_c = 5.0 K), and β-$(BEDT\text{-}TTF)_2IBr_2$ (T_c = 2.8 K). All the Fermi surfaces of the κ-phases can be described in terms of overlapping "distorted circles" and hence are essentially two-dimensional in nature. However, the Fermi surface of the nonsuperconducting κ-phase, κ-$(BMDT\text{-}TTF)_2Au(CN)_2$, exhibits a partial nesting, in contrast to the case of the superconducting κ-phases, which is probably responsible for the metal–insulator transition at ~60 K.

Organic electron-donor molecules derived from tetrathiafulvalene lead to charge-transfer salts that are metals, semiconductors, and superconductors.[1] The superconducting salts formed with bis(ethylenedithio)tetrathiafulvalene (BEDT-TTF or simply ET, **1**) include the β-phase salts β-$(ET)_2X$ ($X^- = I_3^-, AuI_2^-$, and IBr_2^-, for which T_c = 1.4,[2] 5.0,[3] and 2.8 K,[4] respectively), γ-$(ET)_3(I_3)_{2.5}$ (T_c = 2.5 K),[5] θ-$(ET)_2I_3$ (T_c = 3.6 K),[6] and the κ-phase salts κ-$(ET)_2X$ ($X^- = I_3^-$ and $Cu(NCS)_2^-$, for which T_c = 3.6[7] and 10.4 K,[8] respectively). Surprisingly, the *un*symmetrical electron-donor

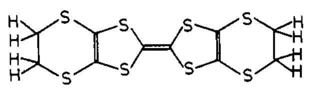

ET
1

[†] North Carolina State University.
[‡] Argonne National Laboratory.
[§] Sandia National Laboratories.

(1) Williams, J. M.; Wang, H. H.; Emge, T. J.; Geiser, U.; Beno, M. A.; Leung, P. C. W.; Carlson, K. D.; Thorn, R. J.; Schultz, A. J.; Whangbo, M.-H. *Prog. Inorg. Chem.* **1987**, *35*, 51.
(2) (a) Yagubskii, E. G.; Shchegolev, I. F.; Laukhin, V. N.; Kononovich, P. A.; Kartsovnik, M. V.; Zvarykina, A. V.; Buravov, L. I. *JETP Lett. (Engl. Transl.)* **1984**, *39*, 12. (b) Williams, J. M.; Emge, T. J.; Wang, H. H.; Beno, M. A.; Copps, P. T.; Hall, L. N.; Carlson, K. D.; Crabtree, G. W. *Inorg. Chem.* **1984**, *23*, 2558.
(3) Wang, H. H.; Beno, M. A.; Geiser, U.; Firestone, M. A.; Webb, K. S.; Nuñez, L.; Crabtree, G. W.; Carlson, K. D.; Williams, J. M.; Azevedo, L. J.; Kwak, J. F.; Schirber, J. E. *Inorg. Chem.* **1985**, *24*, 2465.
(4) Williams, J. M.; Wang, H. H.; Beno, M. A.; Emge, T. J.; Sowa, L. M.; Copps, P. T.; Behroozi, F.; Hall, L. N.; Carlson, K. D.; Crabtree, G. W. *Inorg. Chem.* **1984**, *23*, 3839.
(5) Shibaeva, R. P.; Kaminskii, V. F.; Yagubskii, E. B. *Mol. Cryst. Liq. Cryst.* **1985**, *119*, 361.
(6) Kobayashi, H.; Kato, R.; Kobayashi, A.; Nishio, Y.; Kajita, K.; Sasaki, W. *Chem. Lett.* **1986**, 789.

0020-1669/89/1328-4516$01.50/0

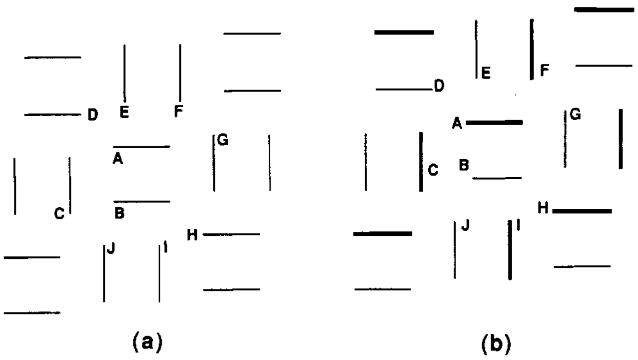

Figure 1. Schematic projection views (along the direction of the central C═C bond of a donor) of how donor dimers pack in the κ-phase salts: (a) κ-(ET)$_2$I$_3$, κ-(MD)$_2$AuI$_2$, κ-(MT)$_2$Au(CN)$_2$; (b) κ-(ET)$_2$Cu(NCS)$_2$. The lables A through J refer to donor molecules.

(methylenedithio)tetrathiafulvalene (MDT-TTF or simply MD, **2**) also gives rise to a superconducting κ-phase salt, κ-(MD)$_2$AuI$_2$

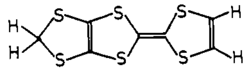

MD

2

(T_c = 4.5 K),[9] while symmetrical donor bis(methylenedithio)tetrathiafulvalene (BMDT-TTF or simply MT, **3**) leads to a

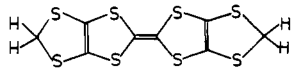

MT

3

nonsuperconducting κ-phase salt, κ-(MT)$_2$Au(CN)$_2$.[10] The latter undergoes a metal–insulator (MI) transition at ~60 K[10] and does not become superconducting even though this MI transition is suppressed by pressure.[11]

Table I. HOMO–HOMO Interaction Energies (β_{ij} in eV) in κ-Phase Salts

pair i–j	κ-(ET)$_2$Cu(NCS)$_2$	κ-(ET)$_2$I$_3$	κ-(MD)$_2$AuI$_2$	κ-(MT)$_2$Au(CN)$_2$
A–B	0.385	0.334	0.451	0.689
B–C[a]	0.198	0.157	0.096	0.258
A–G[b]	0.179	0.157	0.096	0.258
A–C[c]	0.046	0.065	0.074	0.018
B–G[d]	0.038	0.065	0.074	0.018
A–D[e]	0.136	0.105	0.258	0.144

[a] Equivalent to A–E. [b] Equivalent to B–I. [c] Equivalent to A–F. [d] Equivalent to B–J. [e] Equivalent to B–H, C–J, and F–G.

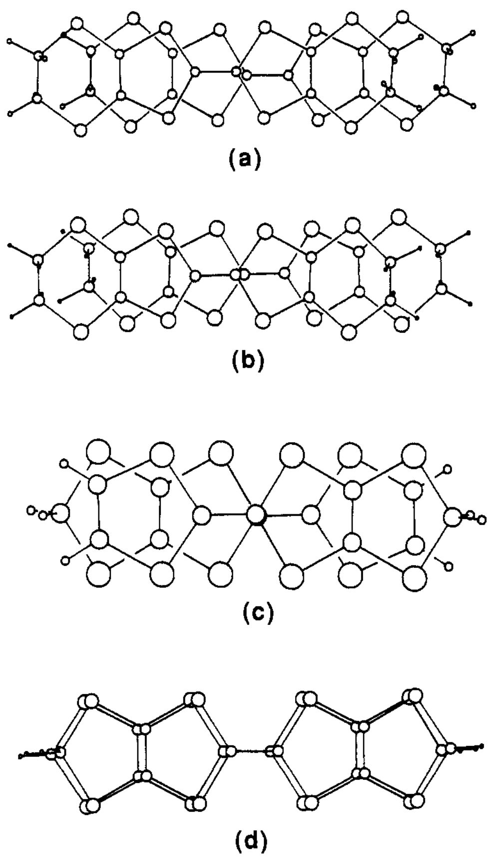

Figure 2. Projection views of donor dimers in (a) κ-(ET)$_2$Cu(NCS)$_2$, (b) κ-(ET)$_2$I$_3$, (c) κ-(MD)$_2$AuI$_2$, and (d) κ-(MT)$_2$Au(CN)$_2$.

The T_c's of the β-phase superconducting salts exhibit interesting trends;[12-15] viz., that of β-(ET)$_2$I$_3$ decreases gradually with increasing applied pressure P when $P < 0.5$ kbar.[14,15] When P reaches ~0.5 kbar, the T_c jumps to ~8 K[14,15] [hence, β-(ET)$_2$I$_3$ with T_c = ~8 K under pressure is referred to as β^*-(ET)$_2$I$_3$, because it is structurally unique],[26] and further increase of P beyond 0.5 kbar gradually lowers T_c from ~8 K (e.g., to ~5 K at P = 3 kbar).[14,15] On the other hand, the T_c's of β-(ET)$_2$AuI$_2$ and β-(ET)$_2$IBr$_2$ decrease gradually with increasing P (e.g., the T_c of β-(ET)$_2$AuI$_2$ becomes ~2 K at P = 3 kbar)[14,15] and do not form high-T_c β^*-salts. A key to understanding these seemingly complicated behaviors of the β-phase superconductors was found to be the relative "softness" of their crystal lattices,[16] which derive from important structural parameters such as short donor···donor and donor···anion contacts involving the terminal C–H bonds of the donor molecules.[16]

---

(7) Kobayashi, A.; Kato, R.; Kobayashi, H.; Moriyama, S.; Nishio, Y.; Kajita, K.; Sasaki, W. *Chem. Lett.* **1987**, 459.

(8) (a) Urayama, H.; Yamochi, H.; Saito, G.; Nozawa, K.; Sugano, T.; Kinoshita, M.; Sato, S.; Oshima, K.; Kawamoto, A.; Tanaka, J. *Chem. Lett.* **1988**, *55*. (b) Urayama, H.; Yamochi, H.; Saito, G.; Sato, S.; Kawamoto, A.; Tanaka, A.; Mori, T.; Maruyama, Y.; Inokuchi, H. *Chem. Lett.* **1988**, 463. (c) Gärtner, S.; Gogu, E.; Heinen, I.; Keller, H. J.; Klutz, T.; Schweitzer, D. *Solid State Commun.* **1988**, *65*, 1531. (d) Carlson, K. D.; Geiser, U.; Kini, A. M.; Wang, H. H.; Montgomery, L. K.; Kwok, W. K.; Beno, M. A.; Williams, J. M.; Cariss, C. S.; Crabtree, G. W.; Whangbo, M.-H.; Evain, M. *Inorg. Chem.* **1988**, *27*, 965.

(9) (a) Papavassiliou, G. C.; Mousdis, G. A.; Zambounis, J. S.; Terzis, A.; Hountas, S.; Hilti, B.; Mayer, C. W.; Pfeiffer, J. *Proceedings of International Conference on Science and Technology of Synthetic Metals*, Santa Fe, NM, June 26–July 2, 1988; *Synth. Met.* **1988**, *27*, B379. (b) Kini, A. M.; Beno, M. A.; Son, D.; Wang, H. H.; Carlson, K. D.; Porter, L. C.; Welp, U.; Vogt, B. A.; Williams, J. M.; Jung, D.; Evain, M.; Whangbo, M.-H.; Overmyer, D. L.; Schirber, J. E. *Solid State Commun.* **1989**, *69*, 503.

(10) Nigrey, P. J.; Morosin, B.; Kwak, J. F.; Venturini, E. L.; Baughman, R. J. *Synth. Met.* **1986**, *16*, 1.

(11) Nigrey, P. J.; Morosin, B.; Kwak, J. F. In *Novel Superconductivity*; Wolf, S. A.; Kresin, V. Z., Eds.; Plenum: New York, 1987; p 171.

(12) (a) Williams, J. M.; Wang, H. H.; Beno, M. A.; Emge, T. J.; Sowa, L. M.; Copps, P. T.; Behroozi, F.; Hall, L. N.; Carlson, K. D.; Crabtree, G. W. *Inorg. Chem.* **1984**, *23*, 3839. (b) Carlson, K. D.; Crabtree, G. W.; Hall, L. N.; Behroozi, F.; Copps, P. T.; Sowa, L. M.; Nuñez, L.; Firestone, M. A.; Wang, H. H.; Beno, M. A.; Emge, T. J.; Williams, J. M. *Mol. Cryst. Liq. Cryst.* **1985**, *125*, 159.

(13) (a) Wang, H. H.; Beno, M. A.; Geiser, U.; Firestone, M. A.; Webb, K. S.; Nuñez, L.; Crabtree, G. W.; Carlson, K. D.; Williams, J. M.; Azevedo, L. J.; Kwak, J. F.; Schirber, J. E. *Inorg. Chem.* **1985**, *24*, 2465. (b) Carlson, K. D.; Crabtree, G. W.; Nuñez, L.; Wang, H. H.; Beno, M. A.; Geiser, U.; Firestone, M. A.; Webb, K. S.; Williams, J. M. *Solid State Commun.* **1986**, *57*, 89.

(14) (a) Laukhin, V. N.; Kostyuchenko, E. E.; Sushko, Yu. V.; Shchegolev, I. F.; Yagubskii, E. B. *JETP Lett.* (*Engl. Transl.*) **1985**, *41*, 81. (b) Murata, K.; Tokumoto, M.; Anzai, H.; Bando, H.; Saito, G.; Kajimura, K.; Ishiguro, T. *J. Phys. Soc. Jpn.* **1985**, *54*, 1236.

(15) (a) Schirber, J. E.; Azevedo, L. J.; Kwak, J. F.; Venturini, E. L.; Leung, P. C. W.; Beno, M. A.; Wang, H. H.; Williams, J. M. *Phys. Rev. B: Condens. Matter* **1986**, *33*, 1987. (b) Schirber, J. E.; Azevedo, L. J.; Kwak, J. F. Venturini, E. L.; Beno, M. A.; Wang, H. H.; Williams, J. M. *Solid State Commun.* **1986**, *59*, 525.

(16) (a) Whangbo, M.-H.; Williams, J. M.; Schultz, A. J.; Emge, T. J.; Beno, M. A. *J. Am. Chem. Soc.* **1987**, *109*, 90. (b) Whangbo, M.-H.; Williams, J. M.; Schultz, A. J.; Beno, M. A. In *Organic and Inorganic Low-Dimensional Crystalline Materials*; Delhaes, P.; Drillon, M., Eds.; Plenum: New York, 1987; p 333.

Figure 3. Schematic projection views (along the direction perpendicular to the central C=C bond of a donor) of how donor molecule planes are arranged with respect to the donor molecule layer: (a) inclined arrangement in κ-$(ET)_2X$ (X^- = $Cu(NCS)_2^-$, I_3^-); (b) perpendicular arrangement in κ-$(MD)_2AuI_2$ and κ-$(MT)_2Au(CN)_2$.

In the present work we investigate the similarities and differences in the structural and electronic properties of the four κ-phase salts κ-$(ET)_2X$ (X^- = $Cu(NCS)_2^-$, I_3^-), κ-$(MD)_2AuI_2$, and κ-$(MT)_2Au(CN)_2$. We examine the structural properties by comparing the donor molecule packing patterns, donor···donor interactions, and donor···anion interactions and compare the electronic properties by calculating the HOMO–HOMO interaction energies,[17] band electronic dispersion relations,[18,19] and Fermi surfaces on the basis of the extended Hückel method.[20] The central objectives of our study are to analyze what structural and electronic aspects separate the nonsuperconducting κ-$(MT)_2Au(CN)_2$ from the superconducting κ-phases, κ-$(ET)_2X$ (X^- = $Cu(NCS)_2^-$, I_3^-) and κ-$(MD)_2AuI_2$, and also to probe whether or not the two "high-T_c" salts ($T_c > 8$ K), κ-$(ET)_2Cu(NCS)_2$ and β^*-$(ET)_2I_3$, have any common structural and electronic features that may serve as a guide to the synthesis of new high-T_c salts.

Crystal Packing

A. Donor Layer. As schematically shown in Figure 1, the donor layers of the κ-phase salts have an "orthogonal" packing of donor dimers. Two molecules of a dimer are slightly different in κ-$(ET)_2Cu(NCS)_2$ but are identical in the other κ-phase salts. The spacing between molecules within a dimer (i.e., the intradimer spacing) is 3.64 Å for nonsuperconducting κ-$(MT)_2Au(CN)_2$, which is substantially greater than the 3.35 Å found for the other κ-phase (superconducting) salts. The extent of interaction between adjacent donor molecules i and j may be measured in terms of their HOMO–HOMO interaction energy[17] $\beta_{ij} = \langle\psi_i|H^{eff}|\psi_j\rangle$, where ψ_i and ψ_j are the HOMO's of donor molecules i and j, respectively. Table I lists the β_{ij} values calculated for various pairs of nearest-neighbor donor molecules defined in Figure 1. In general, the trend in the β_{ij} values is similar, with the largest one found for molecules within a dimer (i.e., β_{AB}). Nevertheless, it is surprising that β_{AB} is largest for κ-$(MT)_2Au(CN)_2$, which has the largest intradimer spacing. Figure 2 shows the projection views of the molecular dimer along the direction perpendicular to the donor molecule plane. Although they are all κ-phase salts, it is noted that donor molecules have a bond-over-bond arrangement in nonsuperconducting κ-$(MT)_2Au(CN)_2$ but a bond-over-ring arrangement in the other κ-phase (superconducting) salts. The bond-over-bond arrangement provides better overlap between the HOMO's, which are π-orbitals, than does the bond-over-ring arrangement. Thus, β_{AB} is largest for κ-$(MT)_2Au(CN)_2$ although it has the greatest intradimer spacing.

As schematically shown in Figure 3a, donor molecule planes are inclined with respect to the donor layer in κ-$(ET)_2X$ (X^- = $Cu(NCS)_2^-$, I_3^-), which is caused by the bond-over-ring arrangement of ET dimers in the two salts. In contrast, κ-$(MD)_2AuI_2$ and κ-$(MT)_2Au(CN)_2$ have their donor molecule planes perpendicular to the donor layer, as schematically shown in Figure 3b. For κ-$(MT)_2Au(CN)_2$ this originates from the bond-over-bond arrangement of the MT dimers. Although a MD dimer has a bond-over-ring arrangement, the two unsymmetrical donor molecules of a dimer are related by inversion symmetry, so that the donor planes are not inclined.

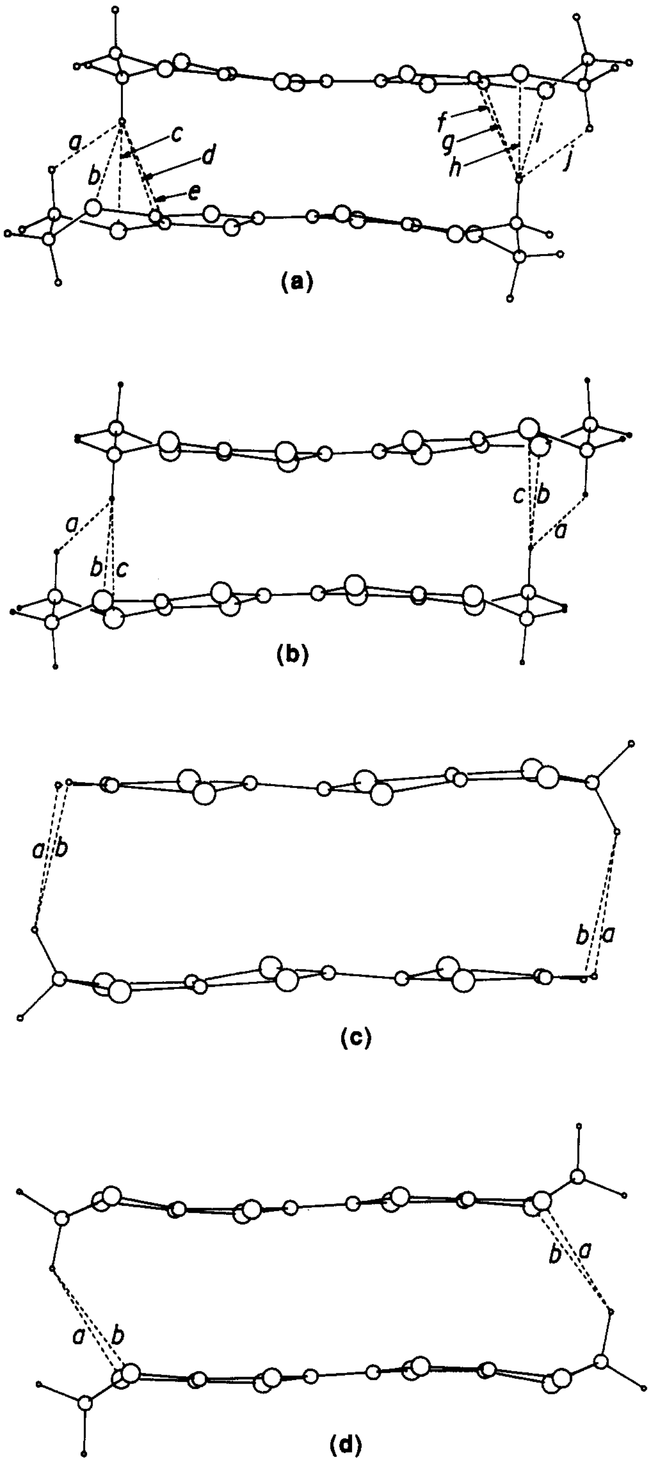

Figure 4. Short intradimer contacts involving the C–H bonds in (a) κ-$(ET)_2Cu(NCS)_2$, (b) κ-$(ET)_2I_3$, (c) κ-$(MD)_2AuI_2$, and (d) κ-$(MT)_2Au(CN)_2$. See Table II for distances.

B. Donor–Donor Interactions Involving C–H Bonds.[21] In most ET salts the six-membered rings of ET adopt the conformation **4a** or **4b**.[22] In **4a** or **4b** the C–H bonds are staggered in each

---

(17) Whangbo, M.-H.; Williams, J. M.; Leung, P. C. W.; Beno, M. A.; Emge, T. J.; Wang, H. H. *Inorg. Chem.* **1985**, *24*, 3500.

(18) Details of our tight-binding-band electronic structure calculations are described in ref 19.

(19) Whangbo, M.-H.; Williams, J. M.; Leung, P. C. W.; Beno, M. A.; Emge, T. J.; Wang, H. H.; Carlson, K. D.; Crabtree, G. W. *J. Am. Chem. Soc.* **1985**, *107*, 5815.

(20) Hoffmann, R. *J. Chem. Phys.* **1963**, *39*, 1397.

(21) In our study, the intermolecular contact distances associated with hydrogen atoms were calculated by using the C_{sp^3}–H and C_{sp^2}–H distances of 1.09 and 1.08 Å, respectively.

(22) Wang, H. H.; Montgomery, L. K.; Geiser, U.; Porter, L. C.; Carlson, K. D.; Ferraro, J. R.; Williams, J. M.; Cariss, C. S.; Rubinstein, R. L.; Whitworth, J. R.; Evain, M.; Novoa, J. J.; Whangbo, M.-H. *Chem. Mater.* **1989**, *1*, 140.

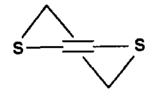

4a

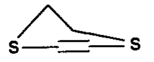

4b

ethylene group, so that two C–H bonds of an ethylene group are roughly perpendicular to the donor molecule plane (i.e., $C-H_{ax}$ bonds), while the other two C–H bonds are approximately parallel to the long axis of ET (i.e., $C-H_{eq}$ bonds). Figure 4a,b also shows the short intradimer contacts involving the $C-H_{ax}$ bonds in κ-$(ET)_2Cu(NCS)_2$ and κ-$(ET)_2I_3$, respectively. Note that a $C-H_{ax}$ bond of one ET is located above one of the two six-membered rings of the other ET molecule. Such $C-H_{ax}$···six-membered ring interactions are absent in the dimers of κ-$(MD)_2AuI_2$ and κ-$(MT)_2Au(CN)_2$, as shown in Figure 4c,d, respectively, because donors MD and MT do not possess $C-H_{ax}$ bonds.

With the conformation **4a**, two six-membered rings of ET may adopt the eclipsed arrangement **5a** or staggered arrangement **5b** (i.e., when viewed along the direction of the central C=C bond of ET, the C—C bonds of the two ethylene groups are eclipsed and staggered in **5a** and **5b**, respectively). ET adopts the staggered ethylene group arrangement **5b** in the "high-T_c" ET salts κ-$(ET)_2Cu(NCS)_2$ (T_c = 10.4 K) and β*-$(ET)_2I_3$ (T_c = ~ 8 K)[16] but the eclipsed arrangement in the "low-T_c" ET salts κ-$(ET)_2I_3$ (T_c = 3.6 K), β-$(ET)_2AuI_2$ (T_c = 5.0 K), and β-$(ET)_2IBr_2$ (T_c = 2.8 K).[16] The T_c's of both β*-$(ET)_2I_3$ and β-$(ET)_2AuI_2$ decrease with increasing an applied pressure P, but, at any given P greater than 0.5 kbar, the T_c of β*-$(ET)_2I_3$ is always higher than that of β-$(ET)_2AuI_2$.[14,15] Therefore, as noted previously,[16] whether the two ethylene groups of ET have a staggered or an eclipsed arrangement is an important structural parameter to consider in understanding the softness of the intermolecular H···H and H···anion contacts and hence the magnitude of the electron–phonon coupling constant. With the eclipsed arrangement **5a**, the short intradimer H···H contact occurs between the "front-side" $C-H_{ax}$ bond of one ET and the "back-side" $C-H_{ax}$ bond of the other ET molecule (e.g., contact *a* in Figure 4b). With the staggered arrangement **5b**, however, the short intradimer H···H contact occurs between the front-side $C-H_{ax}$ bonds of both ET molecules and also between the back-side $C-H_{ax}$ bonds of both ET molecules (e.g., contacts *j* and *a*, respectively, in Figure 4a). Both six-membered rings of ET have the conformation **4a** in the low-T_c ET salt κ-$(ET)_2I_3$ (Figure 4b) and the conformation **4b** in the low-T_c salts β-$(ET)_2X$ (X^- = AuI_2^-, IBr_2^-).[3,4] In the high-T_c salts κ-$(ET)_2Cu(NCS)_2$ and β*-$(ET)_2I_3$, however, one six-membered ring of the ET molecule has the conformation **4a** while the other six-membered ring has the conformation **4b** (Figure 4a). Ab initio SCF–MO/MP2 calculations on a model $C_4S_2H_6$ ring (see **6**) with the 3-21G basis set show[23] that the conformation **4b** is not a minimum-energy structure and is slightly less stable than the

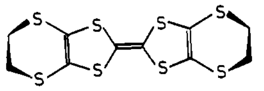

5a

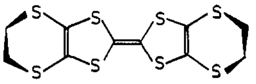

5b

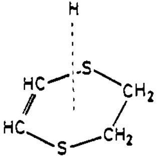

6

minimum-energy conformation **4a** by about 0.61 kcal/mol. In the high-T_c salts κ-$(ET)_2Cu(NCS)_2$ and β*-$(ET)_2I_3$, therefore, one six-membered ring of ET has a stable conformation but the other six-membered ring does not. It is tempting to speculate if such an asymmetrical environment of the ET molecule helps create a lattice instability and therefore enhanced electron–phonon coupling thereby leading to a high T_c. Certainly, the fact that the lattice adopts the ET conformation **4b** means that the crystal packing forces overcome the conformational energy difference between **4a** and **4b**. However, the tendency for the conformational change from **4b** to **4a** could help soften low-frequency translational and/or librational modes of vibration hence increasing the electron–phonon coupling constant and raising the T_c.

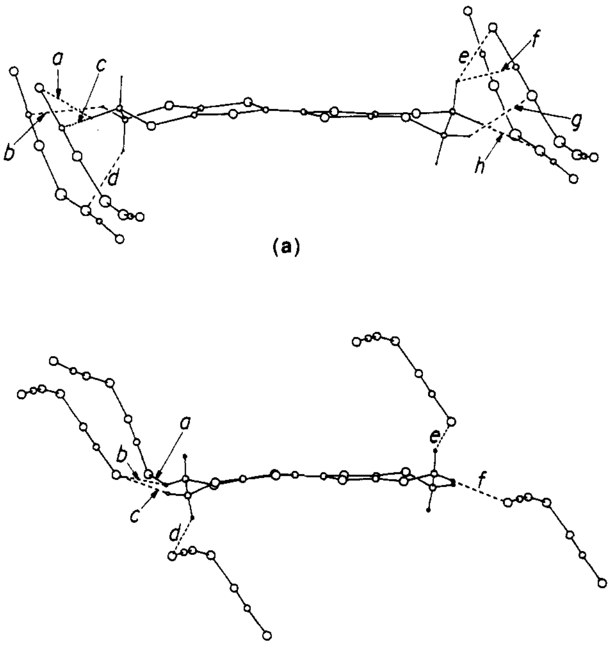

Figure 5. Short donor···anion contacts associated with C–H bonds in κ-$(ET)_2Cu(NCS)_2$: (a) molecule A; (b) molecule B. Distances are given in Table II.

To examine whether the $C-H_{ax}$···six-membered ring interaction of an ET dimer is attractive or repulsive in nature, ab initio SCF–MO/MP2 calculations were performed[23] on the model system, $H_3C-H\cdots C_4S_2H_6$ ring, shown in **6**, where the geometry of the $C_4S_2H_6$ ring was taken from the crystal structure of β*-$(ET)_2I_3$.[26] A CH_4 molecule was placed on top of the $C_4S_2H_6$ ring in such a way that one C–H bond of CH_4, positioned along the direction of the $C-H_{ax}$ bond of the ethylene group lying above the six-membered ring, has the H···H, H···S, and H···C contacts (e.g., their shortest distances are 2.26, 2.90, and 2.85 Å, respectively) as found for the $C-H_{ax}$ bond in β*-$(ET)_2I_3$. With this fixed geometrical arrangement, the $H_3C-H\cdots C_4S_2H_6$ ring interaction is calculated to be attractive by 0.82 kcal/mol at the MP2 level calculations with the 3-21G basis set. Consequently, the $C-H_{ax}$···six-membered ring interactions in ET dimers are expected to be slightly attractive, and this may be partly responsible for the inclined donor-layer structure of ET salts and, in general, their packing motifs.

C. Donor–Anion Interactions. The short calculated C–H···anion contacts associated with the two nonequivalent ET molecules A and B of κ-$(ET)_2Cu(NCS)_2$ are shown in Figure 5a,b, respectively. Molecule A has short C–H···anion contacts primarily with the C and N atoms, while molecule B has short C–H···anion contacts primarily with the S atoms. Therefore, molecules A and B are under what may be termed relatively "hard" and "soft" environments, respectively. This leads to two different –C–C–H bending modes in the polarized infrared reflectance spectra of κ-$(ET)_2Cu(NCS)_2$.[24]

The short C–H···anion contacts of κ-$(ET)_2I_3$, κ-$(MD)_2AuI_2$, and κ-$(MT)_2Au(CN)_2$ are shown in Figure 6a–c, respectively. The

---

(23) Novoa, J. J.; Whangbo, M.-H.; Williams, J. M. Manuscript in preparation.

(24) Ferraro, J. R.; Wang, H. H.; Geiser, U.; Kini, A. M.; Beno, M. A.; Williams, J. M.; Hill, S.; Whangbo, M.-H.; Evain, M. *Solid State Commun.* **1988**, *68*, 917.

(25) Bardeen, J.; Cooper, L. N.; Schrieffer, J. R. *Phys. Rev.* **1957**, *108*, 1175.

(26) Schultz, A. J.; Wang, H. H.; Williams, J. M.; Filhol, A. *J. Am. Chem. Soc.* **1986**, *108*, 7853.

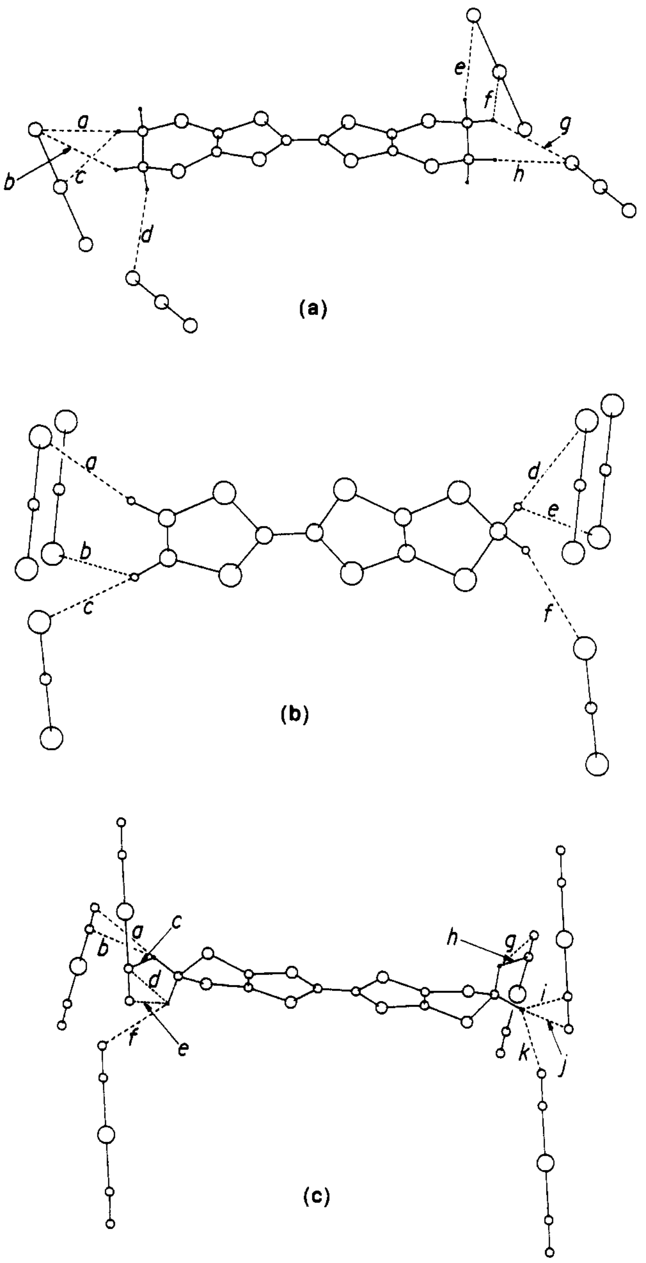

Figure 6. Short donor···anion contacts associated with the C–H bonds in (a) κ-$(ET)_2I_3$, (b) κ-$(MD)_2AuI_2$, and (c) κ-$(MT)_2Au(CN)_2$. Table II contains distances.

shortest calculated H···I and H···H contact distances in κ-$(ET)_2I_3$ (T_c = 3.6 K) are 3.09 and 2.23 Å, respectively, while those in κ-$(MD)_2AuI_2$ (T_c = 4.5 K) are 2.94 and 2.76 Å, respectively. Thus, κ-$(MD)_2AuI_2$ is under a somewhat harder environment than is κ-$(ET)_2I_3$ in terms of the donor–anion interaction (i.e., H···I = 2.94 vs 3.09 Å) but under a much softer environment in terms of the donor–donor interaction (i.e., H···H = 2.76 vs 2.23 Å). This might partially account for the finding that the T_c of κ-$(MD)_2AuI_2$ is slightly higher than that of κ-$(ET)_2I_3$. We do not attempt to compare the short intermolecular contacts for other pairs of κ-phase salts, because the donor molecules and anions involved, particularly the polymeric $Cu(NCS)_2^-$ anion in κ-$(ET)_2Cu(NCS)_2$, are quite different in nature and such comparisons in terms of the relative "softness" of their environments are exceedingly difficult to make. A listing of the important intermolecular contacts in κ-phase salts is given in Table II.

Electronic Structure

A. Dispersion Relations. The dispersion relations of the two highest occupied bands calculated for κ-$(ET)_2Cu(NCS)_2$,[8d] κ-$(ET)_2I_3$, κ-$(MD)_2AuI_2$,[9b] and κ-$(MT)_2Au(CN)_2$ are shown in Figure 7a–d, respectively. Within the dimers of the κ-phase salts, the HOMO's of the donor molecules interact to give the bonding and antibonding levels ψ_+ and ψ_-, respectively. The upper and lower bands of Figure 7 are largely represented by the ψ_- and ψ_+ levels of donor dimers, respectively. Given the formal oxidation state in which every dimer loses one electron, the upper bands of Figure 7 are all half-filled. In general, the band dispersions of the upper and lower bands are similar in all the κ-phase salts. Unlike the case of other κ-phase salts, however, the dispersion of the upper band in κ-$(ET)_2Cu(NCS)_2$ is not degenerate along $M \rightarrow Z$, because two donors of a dimer are not equivalent in this salt.[8d,9b]

The widths of the upper, the lower, and the overall bands (see 7 for definition) of Figure 7 are listed in Table III. These values

Table II. Selected Intermolecular Contact Distances[a] (Å) for κ-Phase Salts with Labels Corresponding to Those Given in Figures 4–6

Interdimer Contacts Involving C–H Bonds					
κ-$(ET)_2Cu(NCS)_2$					
a (H···H)	2.18	*b* (H···S)	3.04	*c* (H···S)	2.99
d (H···C)	2.71	*e* (H···C)	2.74	*f* (H···C)	2.79
g (H···C)	2.75	*h* (H···S)	3.00	*i* (H···S)	3.03
j (H···H)	2.24				
κ-$(ET)_2I_3$					
a (H···H)	2.23	*b* (H···S)	3.67	*c* (H···S)	2.78
κ-$(MD)_2AuI_2$					
a (H···H)	2.76	*b* (H···H)	3.12		
κ-$(MT)_2Au(CN)_2$					
a (H···H)	2.52	*b* (H···S)	3.06	*c* (H···S)	3.28
Donor···Anion Contacts Associated with C–H Bonds					
κ-$(ET)_2Cu(NCS)_2$, Molecule A					
a (H···S)	2.82	*b* (H···C)	2.72	*c* (H···C)	2.97
d (H···N)	2.56	*e* (H···S)	3.01	F (H···C)	2.73
g (H···N)	2.72	*h* (H···N)	2.59		
κ-$(ET)_2Cu(NCS)_2$, Molecule B					
a (H···S)	2.95	*b* (H···S)	2.91	*c* (H···S)	2.72
d (H···S)	3.01	*e* (H···S)	2.93	*f* (H···S)	2.84
κ-$(ET)_2I_3$					
a (H···I)	3.13	*b* (H···I)	3.45	*c* (H···I)	3.09
d (H···I)	3.35	*e* (H···I)	3.73	*f* (H···I)	3.26
κ-$(MD)_2AuI_2$					
a (H···I)	2.94	*b* (H···I)	3.44	*c* (H···I)	3.05
d (H···I)	3.27	*e* (H···I)	3.38	*f* (H···I)	3.02
κ-$(MT)_2Au(CN)_2$					
a (H···N)	2.92	*b* (H···C)	3.10	*c* (H···C)	3.41
d (H···C)	3.24	*e* (H···N)	3.07	*f* (H···N)	2.89
g (H···N)	2.44	*h* (H···C)	2.86	*i* (H···C)	2.54
j (H···N)	2.68	*k* (H···N)	2.87		

[a] Standard deviations involving *calculated* hydrogen atom positions with C–H bond lengths of 1.09 Å (sp^3) and 1.08 Å (sp^2) are on the order of 0.01 Å.

Table III. Superconducting Transition Temperatures, Bandwidths, and Electron Densities of States in the κ-Phase Salts

salt	T_c, K	$n(e_f)$, e/eV	W_l, eV	W_u, eV	W, eV
κ-$(ET)_2Cu(NCS)_2$	10.4	7.57	0.337	0.588	1.066
κ-$(ET)_2I_3$	3.6	7.09	0.349	0.697	1.154
κ-$(MD)_2AuI_2$	4.5	7.98	0.488	0.559	1.157
κ-$(MT)_2Au(CN)_2$		7.30	0.547	0.739	1.692

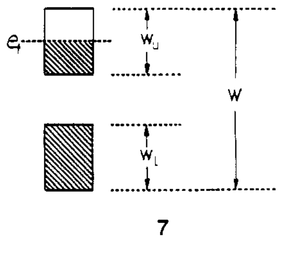

7

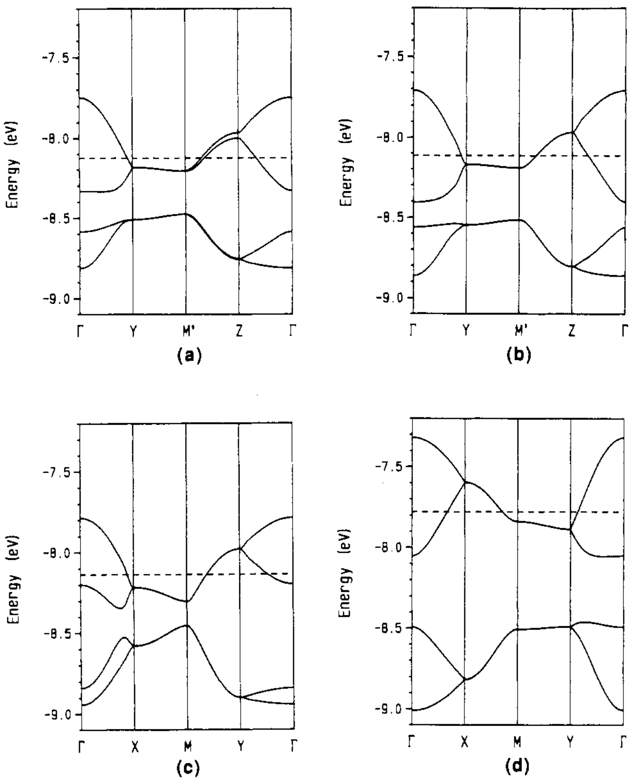

Figure 7. Dispersion relations of the two highest occupied bands calculated for (a) κ-$(ET)_2Cu(NCS)_2$, (b) κ-$(ET)_2I_3$, (c) κ-$(MD)_2AuI_2$, and (d) κ-$(MT)_2Au(CN)_2$. The dashed lines refer to the Fermi levels.

are similar for the superconducting κ-$(ET)_2Cu(NCS)_2$, κ-$(ET)_2I_3$, and κ-$(MD)_2AuI_2$ salts but are somewhat larger for nonsuperconducting κ-$(MT)_2Au(CN)_2$. Also listed in Table III are the calculated electronic densities of states $n(e_f)$ at the Fermi level. Clearly, in the κ-phase salts, a high T_c values does not necessarily correspond to a large $n(e_f)$ value just as in the case of the β-phase ET salts β-$(ET)_2X$ ($X^- = I_3^-$, AuI_2^-, IBr_2^-).[16] Thus, in terms of the bandwidths and $n(e_f)$, the nonsuperconducting salt κ-$(MT)_2Au(CN)_2$ does not appear very different from the superconducting salts κ-$(ET)_2Cu(NCS)_2$, κ-$(ET)_2I_3$, and κ-$(MD)_2AuI_2$. The factor that distinguishes the nonsuperconducting κ-phase salt from the superconducting κ-phase salts is simply the relatively larger (3.64 vs 3.35 Å) intradimer separation. Suppression of the 60 K metal–insulator transition in κ-$(MT)_2Au(CN)_2$ by pressure[11] is consistent with the likely compression of the intradimer distance to that approaching the values found in the superconducting salts.

B. Fermi Surfaces. The Fermi surfaces associated with the half-filled bands of κ-$(ET)_2Cu(NCS)_2$, κ-$(ET)_2I_3$, κ-$(MD)_2AuI_2$, and κ-$(MT)_2Au(CN)_2$ are shown in Figure 8a–d, respectively. Except for the case of κ-$(ET)_2Cu(NCS)_2$, the Fermi surfaces consist essentially of overlapping "distorted circles" centered at Γ and its equivalent points in the κ-space. For κ-$(ET)_2Cu(NCS)_2$, ovelapping circles interact near the crossing points along $M' \rightarrow Z$ and thus are split into wavelike one-dimensional pieces and ellipselike two-dimensional pieces. Except for the noncrossing regions, therefore, the Fermi surface of κ-$(ET)_2Cu(NCS)_2$ is essentially similar to those of the other κ-phase salts. Therefore, all κ-phase salts are expected to be two-dimensional metals. However, we note that the Fermi surface of κ-$(MT)_2Au(CN)_2$ has a shape of an ice rink (see Figure 8d), so that there exists a partial nesting, and the electronic instability resulting from this nesting might be responsible for the metal–insulator transition of κ-$(MT)_2Au(CN)_2$ at 60 K. To investigate the nature of this phase transition, we have tried to determine the crystal structure of κ-$(MT)_2Au(CN)_2$ at a temperature below 60 K. However, our attempt has failed, since this salt undergoes a destructive phase transition under cooling conditions. Further experimental studies are necessary to understand the nature of the metal–insulator phase transition in κ-$(MT)_2Au(CN)_2$.

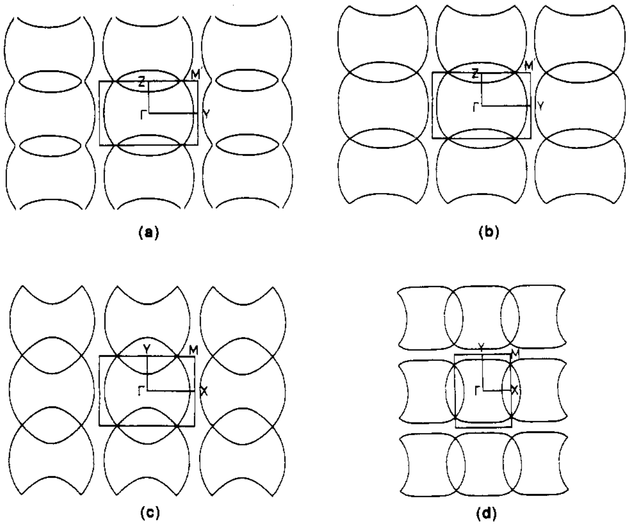

Figure 8. Fermi surfaces associated with the half-filled bands of (a) κ-$(ET)_2Cu(NCS)_2$, (b) κ-$(ET)_2I_3$, (c) κ-$(MD)_2AuI_2$, and (d) κ-$(MT)_2Au(CN)_2$.

Concluding Remarks

Donor molecule dimers of the κ-phase salts have in all of their crystal structures an orthogonal packing arrangement, such that donor "stacks" do not exist in the κ-phase salts compared to the β-phase materials.[1] Nevertheless, all the κ-phase salts have two-dimensional metallic character in their band electronic structures, just as in the case of the β-phase superconducting salts β-$(ET)_2X$ ($X = I_3^-$, AuI_2^-, IBr_2^-), which contain well-formed and interacting donor molecule stacks. In contrast to the Fermi surfaces of the superconducting κ-phases, κ-$(ET)_2X$ ($X^- = Cu(NCS)_2^-$, I_3^-) and κ-$(MD)_2AuI_2$, however, the Fermi surface of the nonsuperconducting κ-phase, κ-$(MT)_2Au(CN)_2$, exhibits a partial nesting, which may in part be responsible for its MI transition at ~60 K. Structurally speaking, κ-$(MT)_2Au(CN)_2$ also differs somewhat from other κ-phase salts in that the donor molecules of a dimer have a bond-over-bond arrangement in κ-$(MT)_2Au(CN)_2$ but a bond-over-ring arrangement in other κ-phase salts. Thus, the intradimer spacing is considerably larger (~3.64 Å) in κ-$(MT)_2Au(CN)_2$ than in other κ-phase salts (~3.35 Å). The Fermi surface anisotropy (i.e., the partial nesting) in κ-$(MT)_2Au(CN)_2$ stems eventually from the bond-over-bond donor arrangement and the large intradimer spacing.

On the basis of a simplified BCS relationship,[25] $T_c \propto \exp[-1/n(e_f)]$, a high T_c is often considered to reflect a large $n(e_f)$. This is not the case in the β-phase superconducting salts β-$(ET)_2X$ ($X^- = I_3^-$, AuI_2^-, IBr_2^-)[16] nor in the κ-phase salts (see Table III). By analogy with the β-phase superconducting salts,[16] the relative lattice "softness" leading to a large electron–phonon coupling constant would be crucial for reaching a high T_c in the κ-phase materials. Since the κ-phase salts are derived from different donor molecules and/or anions, it is difficult to assess the relative softness of their crystal lattices on the basis of structural comparisons. Nevertheless, we note that two terminal ethylene groups of ET have a staggered arrangement in the high-T_c salts κ-$(ET)_2Cu(NCS)_2$ (T_c = 10.4 K) and β*-$(ET)_2I_3$ (T_c = ~8 K) but an eclipsed arrangement in the low-T_c salts κ-$(ET)_2I_3$ (T_c = 3.6 K), β-$(ET)_2AuI_2$ (T_c = 5.0 K), and β-$(ET)_2IBr_2$ (T_c = 2.8 K). In contrast to the case of the low-T_c salts, the two six-membered rings of ET have slightly different conformations in the high-T_c salts. A future goal of our work is to examine if such an asymmetric environment of the ET molecule leads to enhanced electron–phonon coupling and hence a high T_c.

Acknowledgment. Work at Argonne National Laboratory and at North Carolina State University was supported by the Office of Basic Energy Sciences, Division of Materials Sciences, U.S.

Department of Energy, under Contract W-31-109-ENG-38 and Grant DE-FG05-86ER45259, respectively. We express our appreciation for computing time on the ER-Cray X-MP computer, made available by DOE. We wish to thank Professor H. Kobayashi for kindly providing coordinates for the κ-(ET)$_2$I$_3$ salt.

Registry No. κ-(ET)$_2$X (X = Cu(NCS)$_2^-$), 113132-62-0; κ-(ET)$_2$X (X = I$_3^-$), 89061-06-3; κ-(MD)$_2$AuI$_2$, 120389-59-5; κ-(MT)$_2$Au(CN)$_2$, 110899-47-3.

Contribution from the Department of Chemistry and Laboratory for Molecular Structure and Bonding, Texas A&M University, College Station, Texas 77843

Solid-State Geometric Isomers of $Re_2H_8(PPh_3)_4$

F. Albert Cotton* and Rudy L. Luck

Received June 19, 1989

Complexes of the form $Re_2H_8(PR_3)_4$, PR_3 = tertiary-phosphine ligand, have previously been shown in the solid state to be arranged as $(PR_3)_2H_2Re(\mu\text{-}H)_4ReH_2(PR_3)_2$, with the P atoms attached to the adjacent Re atoms being eclipsed (D_{2h} symmetry). The structure of the complex $Re_2H_8(PPh_3)_4$ in the crystalline state is shown here to depend on the solvents used to grow crystals. A crystal form (**1a**) containing a planar eclipsed arrangement, as found previously, consisting of four P and two Re atoms is obtained if hexane is allowed to diffuse slowly into a tetrahydrofuran (THF) solution of the complex. However, a crystal form (**1b**) containing a staggered arrangement of the four P atoms is obtained if crystals are obtained from a saturated solution of $Re_2H_8(PPh_3)_4$ in acetone. The variable-temperature ^1H NMR spectra of this complex in CD_2Cl_2 are also reported. Crystal data: $Re_2H_8(PPh_3)_4\cdot 2C_4H_8O$ (**1a**) (THF/hexane): monoclinic, space group $C2/c$, $a = 20.592$ (9) Å, $b = 17.828$ (4) Å, $c = 18.837$ (4) Å, $\beta = 90.97$ (3)°, $V = 6914$ (4) Å^3, $Z = 4$, $R = 0.0469$ ($R_w = 0.0625$) for 321 parameters and 3822 unique data having $F_o^2 > 3\sigma(F_o^2)$. $Re_2H_8(PPh_3)_4\cdot(CH_3)_2CO$ (**1b**) (acetone): monoclinic, space group $C2/c$, $a = 23.414$ (5) Å, $b = 13.281$ (2) Å, $c = 23.702$ (4) Å, $\beta = 114.84$ (2)°, $V = 6688.4$ (7) Å^3, $Z = 4$, $R = 0.0328$ ($R_w = 0.0464$) for 336 parameters and 4316 unique data having $F_o^2 > 3\sigma(F_o^2)$. **1a** also shows a systematic disordering of 4% of the molecules, from which a possible mechanism (an internal flip of Re_2) for exchange of bridge and terminal hydrogen atoms may be inferred.

Introduction

In 1969 Chatt and Coffey[1] reported two incompletely characterized but extremely interesting compounds, which they tentatively formulated as $[ReH_x(PR_3)_2]_2$. PR_3 was either PEt_2Ph or PPh_3 and x was believed to have a value less than 7. These were called "agnohydrides" because of their uncertain composition and nature. In 1977, Bau et al.[2] reported a neutron diffraction study of the one with PEt_2Ph and showed that it has the composition $Re_2H_8(PEt_2Ph)_4$ and the structure shown schematically in I. In the intervening years, the synthetic procedures[3] for these compounds have been improved, more has been learned about their reaction chemistry,[4-6] and, of particular interest to us, their NMR behavior has been examined.[7] The main features of interest in this last connection are (1) that the bridge and terminal H atoms are rapidly (i.e., on the NMR time scale) undergoing site exchange at room temperature[2,3b,7] and (2) the longitudinal relaxation times (T_1's) for these hydrogen atoms are relatively short at low temperatures.[7]

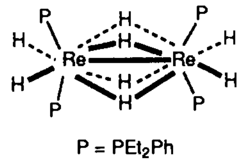

P = PEt_2Ph

I

Table I. Crystallographic Data for $Re_2H_8(PPh_3)_4\cdot 2C_4H_8O$ (**1a**) and $Re_2H_8(PPh_3)_4\cdot(CH_3)_2CO$ (**1b**)

	$C_{80}H_{84}O_2P_4Re_2$ (**1a**)	$C_{75}H_{74}OP_4Re_2$ (**1b**)
fw	1577.81	1511.74
a, Å	20.592 (9)	23.414 (5)
b, Å	17.828 (4)	13.281 (2)
c, Å	18.837 (4)	23.702 (4)
β, deg	90.97 (3)	114.84 (2)
V, Å^3	6914 (4)	6688.4 (7)
Z	4	4
space group	$C2/c$ (No. 15)	$C2/c$ (No. 15)
T, °C	+19	−80
λ, Å	0.71073	0.71073
ρ_{calcd}, g/cm^{-3}	1.516	1.501
μ, cm^{-1}	36.806	38.022
transm coeff	100.00–81.74	99.79–55.65
$R(F_o)^a$	0.0469	0.0328
$R_w(F_o)$	0.0625^b	0.0464^c

[a] $R = \sum||F_o| - |F_c||/\sum|F_o|$. [b] $R_w = [\sum w(|F_o| - |F_c|)^2/\sum w|F_o|^2]]^{1/2}$; $w = 1.3837/[\sigma^2(|F_o|) + 0.001(F_o^2)]$. [c] $R_w = [\sum w(|F_o| - |F_c|)^2/\sum w|F_o|^2]^{1/2}$; $w = 1.1869/[\sigma^2(|F_o|) + 0.001(F_o^2)]$.

Two interesting aspects of these compounds that have not received sufficient attention have been structural studies and the question of how the H_t–H_b exchange may be accomplished. In this paper we report structural results on $Re_2H_8(PPh_3)_4$ (one of the two original agnohydrides) as well as some ideas on the manner in which the remarkably facile H_t–H_b exchange may occur.

Experimental Section

The NMR spectra were recorded in CD_2Cl_2 by using a Varian XL-400 spectrometer. The complex $Re_2H_8(PPh_3)_4$ was obtained in this study either by following the published procedures[1] as a product of the thermal transformation of $ReH_7(PPh_3)_2$ or as a byproduct (27% yield, verified by ^1H NMR relative to $ReH_5(PPh_3)_3$) in an adaptation of a procedure[8]

---

(1) Chatt, J.; Coffey, R. S. *J. Chem. Soc. A* **1969**, 1963.

(2) Bau, R.; Carroll, W. E.; Teller, R. G.; Koetzle, T. F. *J. Am. Chem. Soc.* **1977**, *99*, 3872.

(3) (a) Brant, P.; Walton, R. A. *Inorg. Chem.* **1978**, *17*, 2674. (b) Fanwick, P. E.; Root, D. R.; Walton, R. A. *Inorg. Chem.* **1989**, *28*, 395. (c) Roberts, D. A.; Geoffroy, G. L. *J. Organomet. Chem.* **1981**, *214*, 221.

(4) Allison, J. D.; Walton, R. A. *J. Chem. Soc., Chem. Commun.* **1983**, 401.

(5) Moehring, G. A.; Fanwick, P. E.; Walton, R. A. *Inorg. Chem.* **1987**, *26*, 1861.

(6) Allison, J. D.; Cotton, F. A.; Powell, G. L.; Walton, R. A. *Inorg. Chem.* **1984**, *23*, 159.

(7) (a) Cotton, F. A.; Luck, R. L. *Inorg. Chem.* **1989**, *28*, 6. (b) Cotton, F. A.; Luck, R. L.; Root, D. R.; Walton, R. A. *Inorg. Chem.*, in press.

(8) Douglas, P. G.; Shaw, B. L. *Inorg. Synth.* **1977**, *17*, 64.